

Florida International University FIU Digital Commons

Department of Chemistry and Biochemistry

College of Arts, Sciences & Education

6-26-2015

The Dimerization State of the Mammalian High Mobility Group Protein AT-Hook 2 (HMGA2)

Lorraine Frost

Biomolecular Sciences Institute, Florida International University

Maria A.M. Baez

Biomolecular Sciences Institute and Department of Chemistry and Biochemistry, Florida International University

Christopher Harrilal

Biomolecular Sciences Institute and Department of Chemistry and Biochemistry, Florida International University,
cpharril@fiu.edu

Alyssa Garabedian

Biomolecular Sciences Institute and Department of Chemistry and Biochemistry, Florida International University,
agarabed@fiu.edu

Francisco Fernandez-Lima

Biomolecular Sciences Institute and Department of Chemistry and Biochemistry, Florida International University,
fernandf@fiu.edu

See next page for additional authors

Follow this and additional works at: http://digitalcommons.fiu.edu/chemistry_fac

 Part of the [Life Sciences Commons](#)

Recommended Citation

Frost L, Baez MAM, Harrilal C, Garabedian A, Fernandez-Lima F, Leng F (2015) The Dimerization State of the Mammalian High Mobility Group Protein AT-Hook 2 (HMGA2). PLoS ONE 10(6): e0130478. doi:10.1371/journal.pone.0130478

This work is brought to you for free and open access by the College of Arts, Sciences & Education at FIU Digital Commons. It has been accepted for inclusion in Department of Chemistry and Biochemistry by an authorized administrator of FIU Digital Commons. For more information, please contact dcc@fiu.edu.

Authors

Lorraine Frost, Maria A.M. Baez, Christopher Harrilal, Alyssa Garabedian, Francisco Fernandez-Lima, and Fenfei Leng

RESEARCH ARTICLE

The Dimerization State of the Mammalian High Mobility Group Protein AT-Hook 2 (HMGA2)

Lorraine Frost^{1,2*}, Maria A. M. Baez^{1,2}, Christopher Harrilal^{1,2}, Alyssa Garabedian^{1,2}, Francisco Fernandez-Lima^{1,2}, Fenfei Leng^{1,2*}

1 Biomolecular Sciences Institute, Florida International University, Miami, Florida, United States of America, **2** Department of Chemistry and Biochemistry, Florida International University, Miami, Florida, United States of America

✉ Current address: The Pirbright Institute, Ash Road, Pirbright, Surrey, United Kingdom

* lengf@fiu.edu



OPEN ACCESS

Citation: Frost L, Baez MAM, Harrilal C, Garabedian A, Fernandez-Lima F, Leng F (2015) The Dimerization State of the Mammalian High Mobility Group Protein AT-Hook 2 (HMGA2). PLoS ONE 10(6): e0130478. doi:10.1371/journal.pone.0130478

Editor: Vladimir N. Uversky, University of South Florida College of Medicine, UNITED STATES

Received: March 26, 2015

Accepted: May 20, 2015

Published: June 26, 2015

Copyright: © 2015 Frost et al. This is an open access article distributed under the terms of the [Creative Commons Attribution License](https://creativecommons.org/licenses/by/4.0/), which permits unrestricted use, distribution, and reproduction in any medium, provided the original author and source are credited.

Data Availability Statement: All relevant data are within the paper and its Supporting Information files.

Funding: This work was supported by NIH grants 5SC1HD063059-04 and 1R15GM109254-01A1 (to FL) and R00GM106414 (to FF-L).

Competing Interests: The authors have declared that no competing interests exist.

Abstract

The mammalian high mobility group protein AT-hook 2 (HMGA2) is a chromosomal architectural transcription factor involved in cell transformation and oncogenesis. It consists of three positively charged “AT-hooks” and a negatively charged C-terminus. Sequence analyses, circular dichroism experiments, and gel-filtration studies showed that HMGA2, in the native state, does not have a defined secondary or tertiary structure. Surprisingly, using combined approaches of 1-Ethyl-3-(3-dimethylaminopropyl)carbodiimide hydrochloride (EDC) chemical cross-linking, analytical ultracentrifugation, fluorescence resonance energy transfer (FRET), and mass spectrometry, we discovered that HMGA2 is capable of self-associating into homodimers in aqueous buffer solution. Our results showed that electrostatic interactions between the positively charged “AT-hooks” and the negatively charged C-terminus greatly contribute to the homodimer formation.

Introduction

The mammalian high mobility group protein AT-hook 2 (HMGA2) is a nonhistone chromosomal protein expressed almost exclusively in undifferentiated mesenchymal cells [1]. Disruption of the normal expression pattern of HMGA2 causes deregulation of the cell growth and development [1,2]. Work from Chada’s laboratory showed that *Hmga2* knock-out mice developed pygmy phenotype [1]. These mutant mice were severely deficient in fat cells and other mesenchymal tissues. The same group also demonstrated that disruption of *Hmga2* gene caused a dramatic reduction in obesity of leptin-deficient mice (*Lep^{ob}/Lep^{ob}*) in a gene dosage dependent manner: *Hmga2^{+/+} Lep^{ob}/Lep^{ob}* mice weighed over three times more than *Hmga2^{-/-} Lep^{ob}/Lep^{ob}* animals, and the weight of *Hmga2^{+/-} Lep^{ob}/Lep^{ob}* mice was in between [3]. These results suggest that HMGA2 plays an important role in fat cell proliferation and may be a target for the treatment of obesity [3,4]. HMGA2 was also directly linked to oncogenesis [5–7]. Aberrant expression of the protein has been attributed to the formation of various tumors. These

tumors include benign tumors, such as lipomas [8], uterine leiomyomas [9], and fibroadenomas [10], and malignant tumors, such as lung cancer [11–13], breast cancer [14], prostate cancer [15], and leukemia [16]. Interestingly, the expression level of HMGA2 often correlates with the degree of malignancy, the existence of metastasis, and a poor prognosis [17,18]. These results suggest that HMGA2 is a potential therapeutic target of anti-cancer drugs [19,20]. Additionally, more recent studies showed that HMGA2 was involved in human height [21,22], stem cell youth [23], and human intelligence [24]. The multi-functionalities of HMGA2 make it one of the most intriguing proteins studied so far.

HMGA2 is an architectural transcription factor [25] that binds to and modulates DNA conformation, thus providing a framework for subsequent transcriptional activities. It binds to AT-rich DNA sequences using three “AT-hook” DNA binding domains that contain a unique palindrome sequence, PRGRP, flanked on each side by one or two positively charged amino acid residues [26,27]. The DNA binding domain, in the absence of DNA, is unstructured [28,29]. However, when it binds to the minor groove of AT-rich DNA sequences, it adopted a defined conformation [27,28]. This disordered-to-ordered structural transition provides a unique opportunity for it adapting to different AT-rich DNA context and participating in various nuclear activities [6]. More recently, utilizing a PCR-based systematic evolution of ligands by exponential enrichment (SELEX) procedure, we identified two consensus sequences for HMGA2: 5'-ATATTCGCGAWWATT-3' or 5'-ATATTGCGCAWWATT-3', where W is A or T [30]. Our results showed that the three segments in the consensus sequences (two AT-rich segments and one GC-rich segment) are required for high-affinity binding; mutations of these sequences significantly reduced the DNA binding affinity of HMGA2. These results indicate that HMGA2 does not randomly recognize any AT-rich sequences. In contrast, it binds and bends specific AT-rich DNA sequences [30,31].

One intriguing feature of HMGA2 is the asymmetric charge distribution over its primary structure. In solution, HMGA2 may self-associate to homodimers or homooligomers through electrostatic interactions, and may bind to DNA as a homodimer. In this paper we employed a combination of biophysical and biochemical approaches demonstrating that HMGA2, an intrinsically disordered/unstructured protein (IDP), is capable of self-associating into homodimers in aqueous buffer solution.

Materials and Methods

Proteins and reagents

HMGA2 was purified as described previously [26]. The mutant proteins HMGA2 Δ 95–108 and C41G were made by a PCR-based site directed mutagenesis and purified as described previously [26]. A peptide containing the negatively charged C-terminus (H-CETEETSSQESAEED-OH), therefore named the C-terminal peptide (CTP), was custom-synthesized by Advanced ChemTech, Inc. Tetramethylrhodamine-5-maleimide (TMR), fluorescein-5-maleimide (FM), and tris-(2-carboxyethyl)phosphine hydrochloride (TCEP) were from Molecular Probes, Inc. Sephacryl S-100 HR and low molecular weight gel filtration calibration kit were from Amersham Biosciences. 1-ethyl-3-[3-dimethylaminopropyl]carbodiimide hydrochloride (EDC) was from Pierce Biotechnology, Inc.

Circular dichroism (CD) spectra

Solutions containing 10 μ M of HMGA2 in BPES buffer (6 mM Na₂HPO₄, 2 mM NaH₂PO₄, 1 mM Na₂EDTA, and 185 mM NaCl, pH 7.0) were used for CD measurement. CD spectra were recorded at 24°C on a Jasco J-720 spectropolarimeter. The molar ellipticity ($[\theta]$) was

calculated from the equation $[\theta] = 100\theta/cl$, where θ is the measured ellipticity in degree, c is the concentration, and l is the path length. $\Delta\epsilon$ was calculated from the equation $[\theta] = 3298\Delta\epsilon$.

EDC chemical cross-linking experiments

HMGA2 was dialyzed extensively against MES buffer (10 mM MES, pH 5.5, 50 mM NaCl) and then incubated with 2 mM or the indicated amount of freshly made EDC for 2 hours at 24°C. The reaction was stopped by adding β -mercaptoethanol (20 mM, final concentration) or Tris base (100 mM, final concentration). The protein samples were purified using a pre-equilibrated Sephadex G-50 gel filtration column and analyzed by electrophoresis in 15% SDS-PAGE gels.

Gel filtration experiments

Proteins were resolved in a Sephacryl S-100 HR filtration column (1×50 cm) equilibrated with BPES buffer. The experiments were performed at 24°C using gravitational force to elute the proteins. A low molecular weight gel filtration calibration kit containing five protein standards, ribonuclease A (M_w , 13,700), chymotrypsinogen A (M_w , 25,000), ovalbumin (M_w , 43,000), albumin (M_w , 67,000), and Blue Dextran 2000 was used to calibrate the column in three different runs. The fractions at 0.5 ml each were collected; the elution volumes (V_e) of the proteins were determined by UV absorbance. The Stokes radius (R_S) of HMGA2 was estimated from a plot of the V_e of the four standard proteins vs. their Stokes radii (Ribonuclease A, 16.4 Å; Chymotrypsinogen A, 20.9 Å; Ovalbumin, 30.5 Å; Albumin, 35.5 Å). The apparent molecular weight of HMGA2 was also estimated by a similar method. To determine whether the CTP binds to HMGA2 Δ 95–108, the CTP-TMR was incubated with HMGA2 Δ 95–108 for 30 minutes at 24°C, and loaded and resolved by the Sephacryl S-100 HR filtration column (1×50 cm) equilibrated with BPES buffer.

Sedimentation velocity analysis

HMGA2 was equilibrated by dialysis with BPES buffer. Sedimentation velocity experiments were conducted at 20°C in Beckman Instruments XLI located in the National Analytical Ultracentrifugation Facility at the University of Connecticut Biotechnology Center. The program Sednterp [32] was used to calculate the following physical constants: $M_{seq} = 11,819$ Dalton, $\bar{v}_{20^0} = 0.7123$ g/ml, $\rho_{20^0} = 1.00712$ g/ml, and $\eta_{20^0} = 0.01002$ poise, where M_{seq} is the molecular weight calculated from the sequence; \bar{v}_{20^0} , ρ_{20^0} , η_{20^0} are the partial specific volume, the buffer density, and the buffer viscosity, respectively, at 20°C. A stock solution containing 270 μ M of HMGA2 was used to prepare three concentrations of the protein containing, respectively, 135, 45, and 13.5 μ M of HMGA2. These dilutions were then used in a sedimentation velocity run, using the 4-hole rotor at 20°C and 55,000 rpm. Synthetic boundary cells (cuvettes in the center-piece) were loaded with 420 μ l of buffer and 410 μ l of the appropriate sample solution. The cells were placed in the rotor and accelerated to 12,000 rpm while monitoring the transfer of the excess buffer in each cell. Subsequently, the run was stopped and the rotor was gently inverted to thoroughly mix the contents of the cells. The rotor was then equilibrated in a vacuum at 20°C and after a period of 30 min at 20°C the rotor was accelerated to 55,000 rpm. Interference scans were acquired at 1 min intervals for approximately 6 hours. The data was fitted to two programs Sedfit and Sedanal to determine the protein's sedimentation coefficient and molecular weight, which can be used to model the protein's shape using the program Sednterp.

Labeling of HMGA2 and CTP by TMR or FM

Since HMGA2 and the CTP each contain a cysteine residue, they were labeled using TMR or FM. For labeling, 100 μM of HMGA2 or the CTP was incubated with 200 μM TMR or FM in the presence of 400 μM TCEP in 50 mM phosphate buffer (pH 7.2) plus 20 mM NaCl for 2 hours at 24°C. HMGA2-TMR or HMGA2-FM was purified by two consecutive passages through pre-equilibrated Sephadex G-50 spin columns and dialyzed extensively against the buffer used for labeling. To purify the CTP-TMR, the labeling mixture was loaded onto a pre-equilibrated SP-sepharose column (1 ml) and eluted with 50 mM phosphate buffer (pH 7.2) plus 500 mM NaCl. An extinction coefficient of 95,000 $\text{cm}^{-1}\text{M}^{-1}$ at 541 nm in methanol was used to determine the TMR concentration. An extinction coefficient of 83,000 $\text{cm}^{-1}\text{M}^{-1}$ at 492 nm in Tris-HCl (pH 9.0) was used to determine the FM concentration.

Steady-State Fluorescence Measurements

Fluorescence spectra of HMGA2-FM were acquired using a Jobin Yvon FluoroMax-3 spectrofluorometer with excitation wavelength of 492 nm. In the fluorescence resonance energy transfer (FRET) titration experiment, 20 nM of HMGA2-FM in Tris buffer (50 mM Tris-HCl (pH 8.0), 50 or 200 mM NaCl) was titrated by increasing concentrations of HMGA2-TMR. The fluorescence spectra were recorded from 500 to 600 nm.

Trapped Ion Mobility Spectrometry—Mass spectrometry studies (TIMS-MS)

Details regarding the TIMS operation and specifics compared to traditional IMS can be found elsewhere [33–37]. Briefly, in TIMS mobility separation is based on holding the ions stationary using an electric field against a moving gas. The separation in a TIMS device can be described by the center of the mass frame using the same principles as in a conventional IMS drift tube [38]. The TIMS analyzer was coupled to a maXis Impact Q-UHR-ToF (Bruker Daltonics Inc., Billerica, MA). Data acquisition was controlled using in-house software, written in National Instruments Lab VIEW (2012, v. 12.0f3), and synchronized with the maXis Impact acquisition program. TIMS separation was performed using nitrogen as a bath gas at ca. 300 K and typical P_1 and P_2 values are 2.6 and 1.0 mbar, respectively. The same RF (880 kHz and 200–350 V_{pp}) was applied to all electrodes including the entrance funnel, the mobility separating section, and the exit funnel. Protein samples were prepared at 1, 10, 50 and 100 μM concentration using HPLC grade solvents from Thermo Fisher Scientific Inc. (Waltham, MA). An electrospray ionization source (ESI, Bruker Daltonics Inc., MA) was used for all analyses in positive ion mode.

Results

HMGA2 is an intrinsically disordered/unstructured protein (IDP)

Mouse HMGA2 is a 108 amino acid residue protein. Inspection of its primary structure gives some unique features. It has 25 basic amino acid residues (either Lys or Arg), 12 acidic amino acid residues (either Glu or Asp), 15 Pro, and 10 Gly. The high contents of the basic amino acid residues make HMGA2 a high isoelectric point protein (the isoelectric point was estimated to be about 11; the estimated net charge at pH 7.0 is about +13). The charge distribution of HMGA2 is asymmetrical, with the positively charged residues mainly concentrated in the center of the sequence and the negatively charged residues at the C-terminus (Fig 1A). Several programs, such as PONDR [39], DISOPRED [40], and GlobPlot [41], were used to predict its secondary structure. All predicted that HMGA2 in the native state does not adopt a defined structure. Indeed, our CD studies showed that HMGA2 is an unstructured protein. Fig 1B

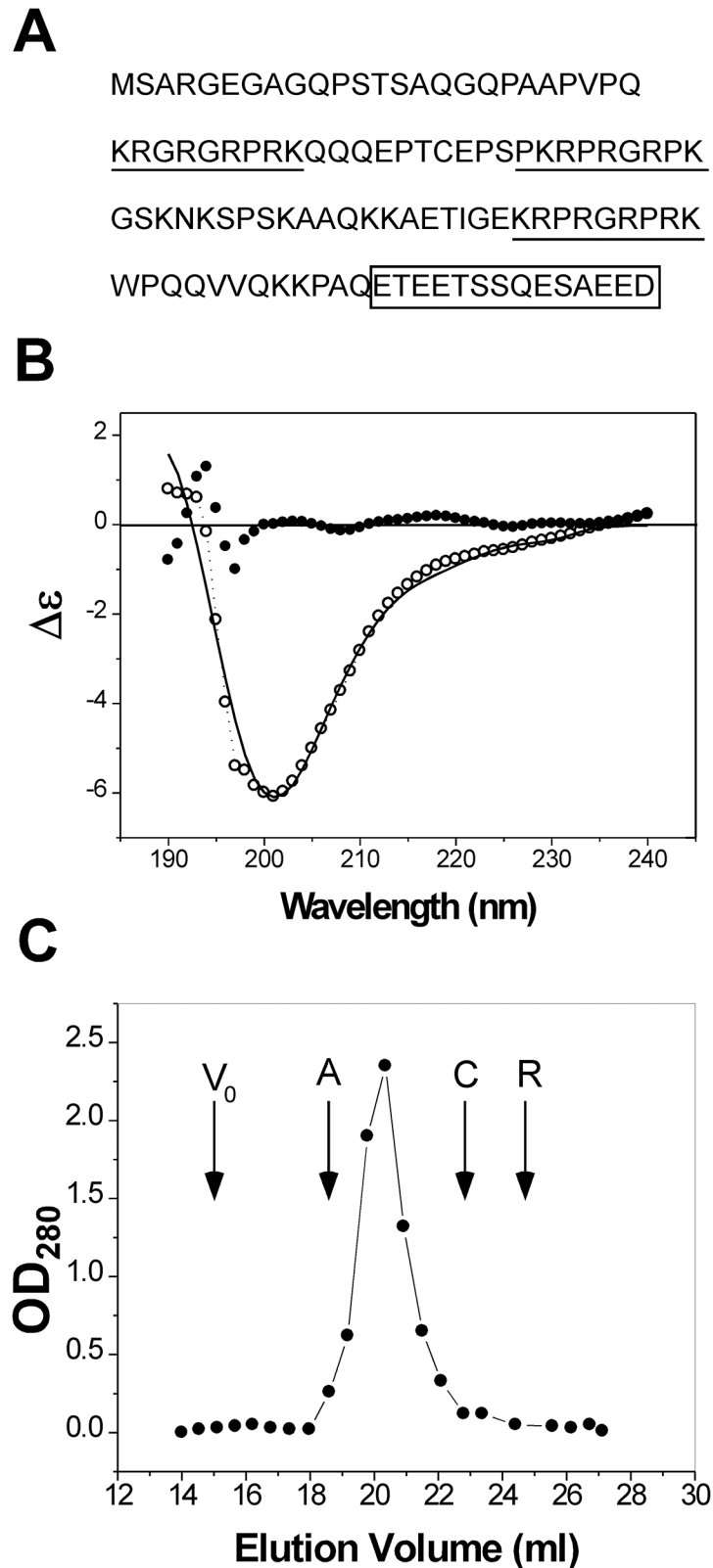


Fig 1. (A) Amino acid sequence of mouse HMGA2. The positively charged “AT hooks” and the negatively charged C-terminus are highlighted by underlines and a box, respectively. **(B) The experimental (open dots with dotted line) and calculated (solid line) CD spectra of HMGA2 in BPES buffer.** The CD spectra were

calculated by the program CONTIN as described in the text. The solid dots are residuals. **(C) Gel filtration chromatography profile of HMGA2 in solution.** Recombinant HMGA2 was resolved by gel filtration in the Sephacryl S-100 column as described under "Materials and Methods." V_0 is the void volume; A, C, and R represent the elution volume of albumin, chymotrypsinogen A, and ribonuclease A, respectively.

doi:10.1371/journal.pone.0130478.g001

shows the CD spectrum of HMGA2 in which the strong peak near 200 nm indicates an unordered conformation. The CD results were further analyzed using three CD analysis programs CONTIN, CDSSTR, and SELCON3 that are included in a downloadable software package CDPro [42]. These analyses showed that about 80% of HMGA2 is unstructured (Fig 1B; S1 Table, Supplementary data). Interestingly, all programs suggest that HMGA2 has about 20% β -sheet component. It is possible that part of HMGA2 has an extended structure similar to β strands. A comparison of the experimental and calculated CD spectra is shown in Fig 1B. Similar results were obtained in our NMR analyses and DSC experiments [29].

HMGA2 was also studied by gel-filtration experiments. Fig 1C shows the gel filtration profile of HMGA2. We calculated the Stokes radius (R_s) of HMGA2 using globular proteins with known hydrodynamic dimensions as standards. The calculated R_s of 30.2 Å for HMGA2 is much too large for a protein with a molecular weight of 12,000 Daltons. In comparison, the R_s of ribonuclease A, a monomeric globular protein with a similar MW (13,700 Daltons), is 16.4 Å. These results suggest that HMGA2 is either a homodimer (or homo-oligomer) or an extended unfolded non-globular protein or both. The R_s calculated from gel filtration studies is almost the same with that calculated from sedimentation velocity analyses (see below for details). Based on the results discussed above, we conclude that HMGA2 is an IDP. This conclusion is consistent with previous studies, which demonstrated that a similar protein, HMGA1a, is an IDP [28,43].

HMGA2 is a homodimer in aqueous buffer solution

In the process of purifying and characterizing HMGA2, we found that a small amount, but variable of HMGA2 always migrates as a dimeric form on SDS-PAGE gels (data not shown). We also found that HMGA2 readily forms an interstrand disulfide bond through C41 in the absence of a reducing reagent such as β -mercaptoethanol or DTT. Furthermore, HMGA2 aggregates under certain conditions, e.g. at high protein concentrations or in the presence of nucleic acids. As discussed above, one of the unique characteristics of HMGA2 is the asymmetrical charge distribution in the primary structure. We therefore reasoned that the protein might exist as a homodimer or a homo-oligomer in aqueous buffer solution.

The oligomeric state of HMGA2 was first analyzed using EDC chemical cross-linking experiments. EDC is a zero-length cross-linker that reacts with closely contacted carboxyl and amino groups. For proteins, the carboxyl groups come from the side chains of Glu and Asp residues or from the unmodified C-terminus; the amino groups come from the side chains of Lys residue or the unmodified N-terminus. HMGA2 has 11 Glu and 1 Asp residues of which seven are located in the C-terminus (Fig 1A). It also has 13 Lys residues whose amino groups on the side chain can be cross-linked to the carboxyl groups by EDC. Fig 2 is a typical EDC chemical cross-linking experiment in which EDC efficiently cross-linked HMGA2 into homodimers (compare lanes 3–6 with lane 2, approximately 60–70% of HMGA2 was cross-linked into dimers). These results suggest that some residues between the subunits of HMGA2 homodimers are in very close proximity to one another. Interestingly, after the cross-linking reaction, the protein samples still had a significant amount of monomers that migrated faster than the protein in the control lane (compare lane 2 with lanes 3–6 of Fig 2). These results suggest that the negatively charged C-terminus may also interact with other parts of HMGA2 in the same

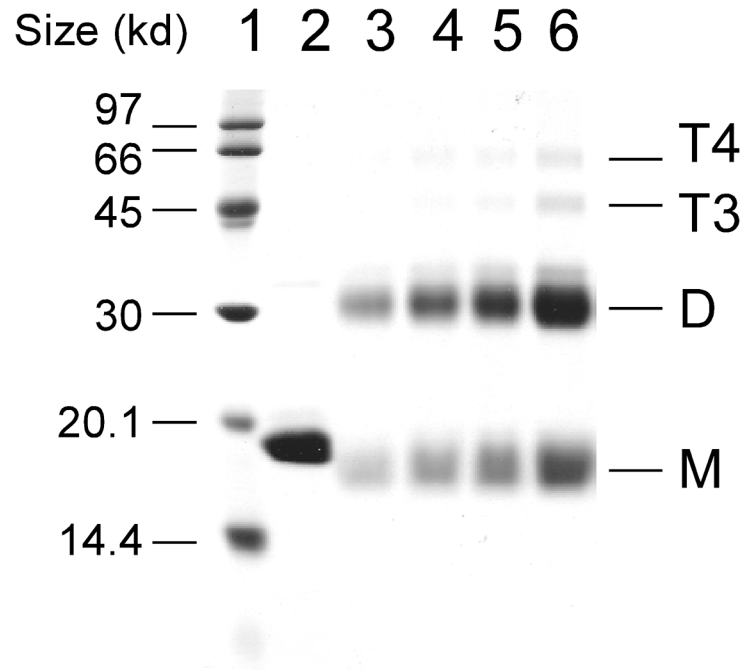


Fig 2. Chemical cross-linking HMGA2 into homodimers with EDC. Chemical cross-linking reactions with EDC in MES buffer were performed as described under “Materials and Methods.” Cross-linked protein samples were analyzed by electrophoresis in a 15% SDS-PAGE gel and stained with Coomassie Brilliant Blue R-250. Lane 1 contained molecular standards; lane 2 contained HMGA2 in the absence of EDC; lanes 3 to 6 contained, respectively, 29, 39, 58, and 116 μM HMGA2 in the presence of 2 mM EDC. M, monomer; D, dimer; T3, trimer; T4, tetramer.

doi:10.1371/journal.pone.0130478.g002

subunit. When the HMGA2 concentration was increased in the cross-linking reactions, other homo-oligomers were also formed (Lanes 4 to 6 of Fig 2; they were assumed to be trimers or tetramers based on migration rates on the SDS-PAGE gels). Ionic strength has no apparent effects on the EDC chemical cross-linking reactions (data not shown). Similar results were obtained using disuccinimidyl suberate (DSS) and dimethyl suberimidate (DMS) as chemical cross-linking reagents that cross-link two primary amines (data not shown). However, the cross-linking efficiency of DSS and DMS is significantly lower than that of EDC. A cysteineless mutant protein, HMGA2C41G, which cannot form a disulfide bond, was also efficiently cross-linked into homodimers by EDC (data not shown).

HMGA2 as a homodimer was confirmed by sedimentation velocity analyses, which may also be used to derive the self-association constant for the dimerization process. Three concentrations of HMGA2, 13.5, 45, and 135 μM were used. The sedimentation velocity data were first individually fitted using two programs Sedfit V8.7 [44] and Sedanal V3.45 [45] using the model of a single non-interacting discrete species. The results of the individual fits are summarized in Table 1 for the program Sedfit and S2 Table (Supplementary data) for the program Sedanal. The slight trend of increasing sedimentation coefficient with increasing concentration may be indicative of either an association reaction taking place, albeit very weak (this result is consistent with our EDC chemical cross-linking studies in which higher oligomers are formed upon increasing the concentration of HMGA2 (Fig 2)), or possible dissociation of the dimer upon dilution. All attempts to fit the data to either an association or dissociation scheme failed. S1 Fig (Supplementary data) shows the individual fit of the time-difference data for three concentrations of HMGA2 using finite-element numerical solutions of the Lamm equation. The

Table 1. Results for individually fitting the sedimentation velocity data to the model of a single ideal species by the program Sedfit (version 8.7).

Concentration (μM)	s (Svedbergs) [95% CI] ^a	Mw (kDa) [95% CI] ^b	RMSD of fit (μM)
13.5	1.641 [1.636, 1.656]	20.6 [19.9, 21.9]	0.15
45	1.682 [1.679, 1.691]	20.5 [20.0, 21.1]	0.26
135	1.705 [1.701, 1.709]	22.1 [21.5, 22.6]	0.82

^aIn this table, s represents the sedimentation coefficient of HMGA2 at 20°C; Mw represents molecular weight; RMSD of fit is the root-mean-square deviation of the fit.

^bValues in parentheses are the 95% confidence interval (CI) for the molecular weight and sedimentation coefficient.

doi:10.1371/journal.pone.0130478.t001

data for all three concentrations was also analyzed globally, i.e. all three data sets fitted simultaneously, using Sedanal V 3.45, which allows the use of fitting models to directly fit the data to various association schemes using multiple data sets. The global fit for the sample datasets to the model of a single ideal species yielded a value for s of 1.711 S [95% confidence intervals: 1.708 S, 1.715 S] and a value for MW of 23.5 kDa. This value for the molecular weight agrees well with that predicted for a homodimer of HMGA2. With the knowledge of s and molecular weight of HMGA2, we predicted that HMGA2 is an elongated, non-globular homodimer (Table 2).

The self-association of HMGA2 was further studied by fluorescence resonance energy transfer (FRET) titration experiment. In this experiment, HMGA2 was labeled with fluorescein-5-maleimide (FM) or tetramethylrhodamin-5-maleimide (TMR) to produce HMGA2-FM or HMGA2-TMR. If HMGA2 self-associates into homodimers or homooligomers, FRET should be detected using the FM donor/TMR acceptor fluorophore pair. Fig 3 shows the fluorescence spectra of HMGA2-FM in the presence of increasing concentrations of HMGA2-TMR for two different salt concentrations, 50 mM (Fig 3A and 3B) and 200 mM NaCl (Fig 3C and 3D). The

Table 2. Hydrodynamic properties of HMGA2 calculated from sedimentation velocity results by program Sednterp.

$s_{20,w}$	1.7731S
^a Mw	23.5 kDa
Hydration	0.4866 g/g
f/f ₀	1.7987
^a R _{Stokes}	3.39 nm
^b Mw	45.0 kDa
^b R _{Stoke}	3.02 nm
Cylindrical model, L	18.024 nm
d	1.823 nm
L/d	9.889

^aThe apparent molecular weight (Mw) and Stokes' radius (R_{Stokes}) of HMGA2 was calculated according to sedimentation velocity studies.

^bThe apparent Mw and R_{Stokes} of HMGA2 were calculated according to gel-filtration results. In this table, we assume that HMGA2 is a cylinder. Two parameters, L, the length of the cylinder and d, the diameter, are required to calculate the hydrodynamic model. The following three equations are used to compute L and d: $s = \frac{M(1-\bar{v})}{N_0 f}$; $f = \frac{3\pi\eta L}{\ln\left\{\frac{L}{d} + \left[0.312 + \frac{0.561d}{L} + 0.1\left(\frac{d}{L}\right)^2\right]}\right\}}$; $V = \frac{M\bar{v}}{N_0\rho} + \frac{M\bar{v}}{N_0} = \pi\left(\frac{d}{2}\right)^2 L$, where M, s, f, \bar{v} , and N₀ are the molecular weight of the solute (protein), the sedimentation coefficient, the friction coefficient, the partial specific volume of the protein, the buffer density, the buffer viscosity, and Avogadro's number, respectively.

doi:10.1371/journal.pone.0130478.t002

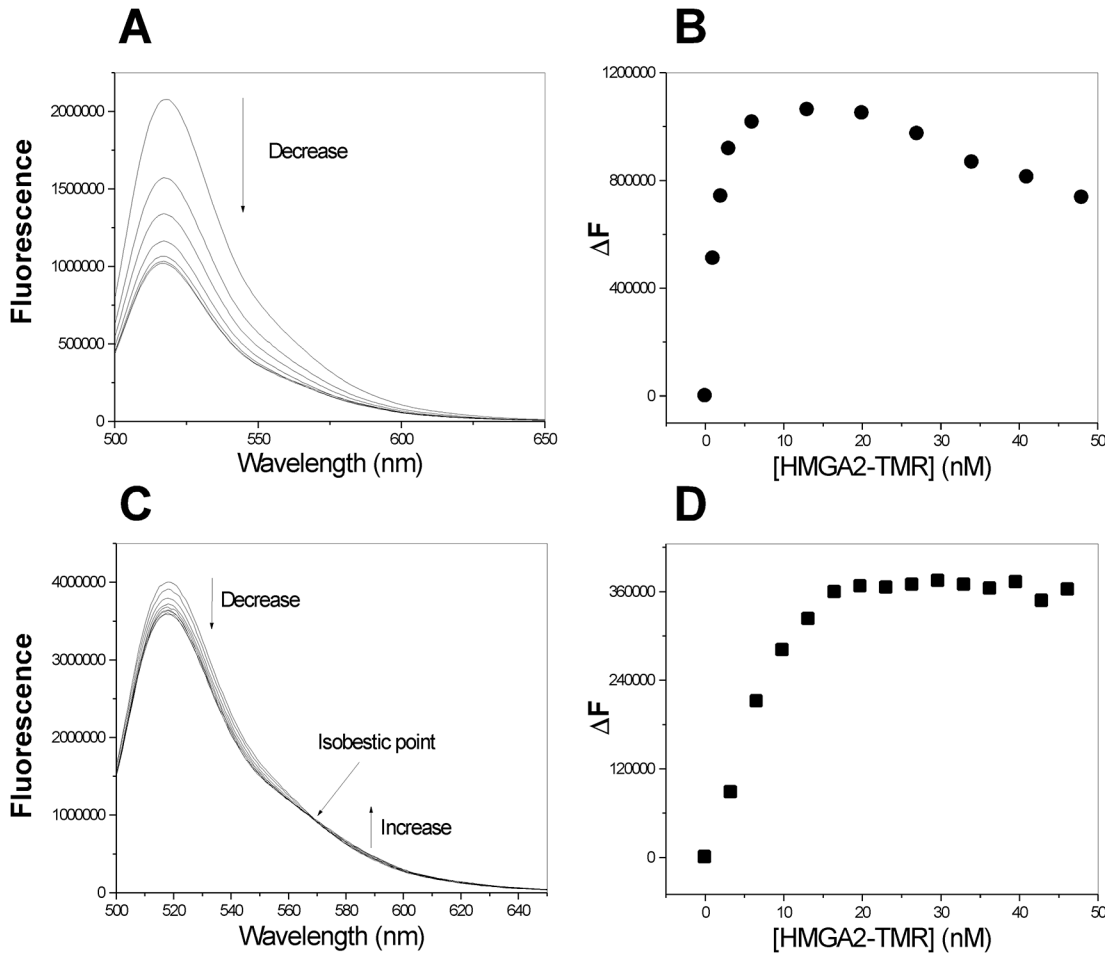


Fig 3. Self-association of HMGA2 was demonstrated by the FRET experiments. (A) and (C), respectively, represent fluorescence spectra of HMGA2-FM in the presence of increasing concentrations of HMGA2-TMR in 50 mM Tris-HCl (pH 8.0) and 50 mM (A) or 200 mM (C) NaCl. (B) and (D) are the difference in fluorescence intensity at 518 nm (ΔF) as a function of HMGA2-TMR concentration was shown for the FRET experiment in panel A and panel C respectively. The fluorescence spectra of HMGA2-FM (20 nM; $\lambda_{excitation} = 492$ nm) were recorded as described under "Materials & Methods."

doi:10.1371/journal.pone.0130478.g003

fluorescence intensity at 518 nm decreased with increasing HMGA2-TMR concentrations. The decrease saturated at high HMGA2-TMR concentration, indicating that HMGA2-TMR binds to HMGA2-FM. Interestingly, we observed some difference between the two FRET experiments. For the FRET experiment in the presence of 50 mM NaCl, the fluorescence decrease saturated at 5 to 10 nM of HMGA2-TMR and increased again after adding more than 20 nM of HMGA2-TMR (Fig 3B). For the FRET experiment in the presence of 200 mM NaCl, the fluorescence decrease saturated at 20 nM of HMGA2-TMR, indicating a 1:1 molar ratio of HMGA2-FM/HMGA2-TMR (Fig 3B). We also observed the fluorescence increase at 588 nm and an isobestic point for the experiment in the presence of 200 mM NaCl (Fig 3C). In addition, we found that the quench magnitude is different. For the 50 mM case, more than 50% of HMGA2-FM fluorescence was quenched by HMGA2-TMR (Fig 3A); for 200 mM case, only about 10% of HMGA2-FM fluorescence was quenched by HMGA2-TMR (Fig 3C). These results suggest that the self-association of HMGA2 is salt-dependent and the electrostatic interaction plays an important role in the self-association process.

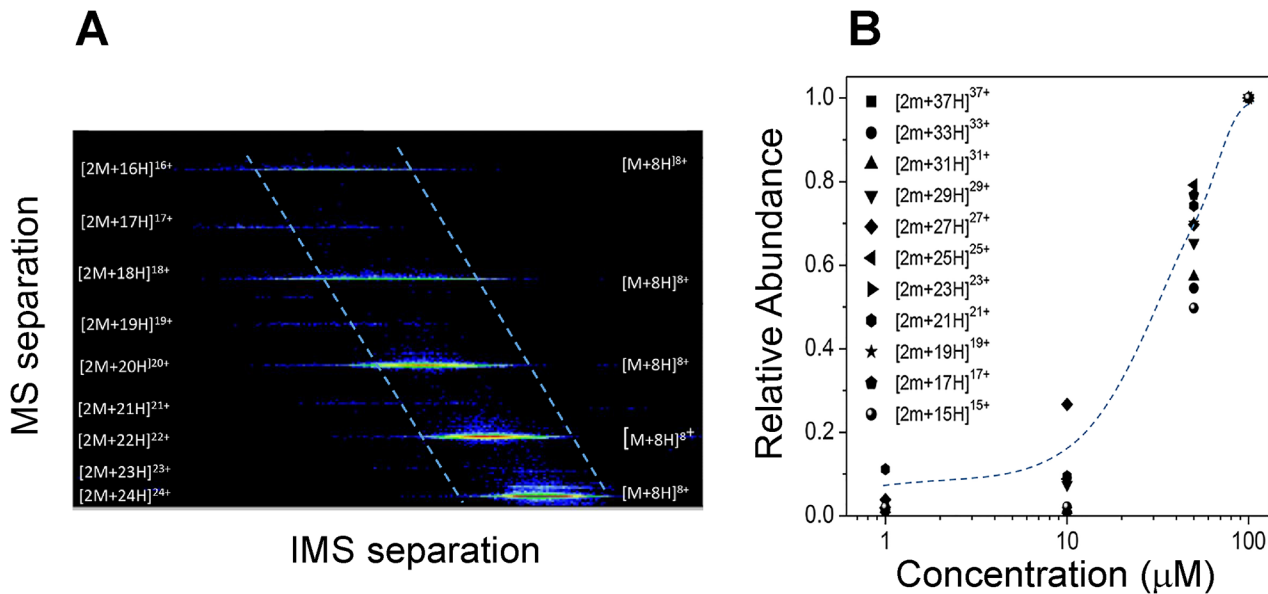


Fig 4. (A) A typical 2D IMS-MS contour plot showing the monomer and dimer signals at 100 μM . Notice the overlap at even charge states in the MS domain for the monomer and dimer peaks. (B) Relative abundance of the dimer formation as a function of the concentration for the odd charge states.

doi:10.1371/journal.pone.0130478.g004

Mass spectrometry studies

The analysis of 2D IMS-MS contour plots (Fig 4) showed the separation in mobility and m/z domains of the $[M+nH]^{+n}$ and $[2M+nH]^{+n}$ monomer and dimer charge state distributions, respectively. Close inspection of the 2D IMS-MS plots shows that for odd charge state of the $[2M+nH]^{+n}$ series, a clear separation of the dimer component can be achieved, since there is no equivalent m/z on the $[M+nH]^{+n}$ monomer series. In addition, the IMS-MS plots permit the measurements of the relative abundance of each series without the interferences from other m/z . Analysis of the relative abundances of the dimer series relative to the monomer series as a function of the protein concentration in the ESI starting solution shows that as the concentration increases, the dimer formation increases. In particular, dimer observation is significant at concentrations larger than 10 μM . While the mechanism of dimer formation may be controversial (i.e., pre-formed in solution or formed during ESI process in the gas-phase), our experimental data from previous experiments (see above) suggest that dimers are pre-formed in solution and remain intact during the ESI process (soft ionization). The lack of trimer, tetramer and higher order oligomers typically observed during ESI condensation at high sample concentration in the IMS-MS data also supports this hypothesis.

The role of the C-terminus in dimer formation

We next investigated what factors are critical to HMGA2 homodimer formation. One possible factor is electrostatic interactions between the positively charged “AT-hooks” and the negatively charged C-terminus. We therefore made a mutant HMGA2 Δ 95–108 that lacks the negatively charged C-terminus, and reasoned that it should not form homodimers. Indeed, our EDC chemical cross-linking experiments showed that HMGA2 Δ 95–108 could not form homodimers (compare lanes 2 & 3 with lanes 5 & 6 of Fig 5). These results suggest that the negatively charged C-terminus is required for the dimer formation. We then, used tetramethylrhodamine-5-maleimide (TMR) to label a 14 amino acid residue C-terminal peptide (the CTP) of

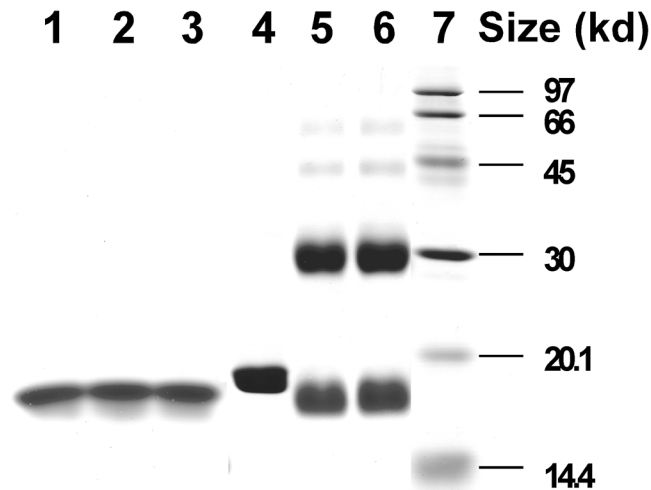


Fig 5. Chemical cross-linking of HMGA2 and HMGA2 Δ 95–108 with EDC. Chemical cross-linking reactions with EDC in MES buffer were performed as described under “Materials and Methods.” Cross-linked protein samples were analyzed by electrophoresis in a 15% SDS-PAGE gel and stained with Coomassie Brilliant Blue R-250. Lane 1 contained HMGA2 Δ 95–108 in the absence of EDC; lanes 2 and 3 contained 40 μ M HMGA2 Δ 95–108 in the presence of 2 mM EDC; lane 4 contained HMGA2 in the absence of EDC; lanes 5 and 6 contained 40 μ M HMGA2 in the presence of 2 mM EDC; lane 7 contained molecular standards.

doi:10.1371/journal.pone.0130478.g005

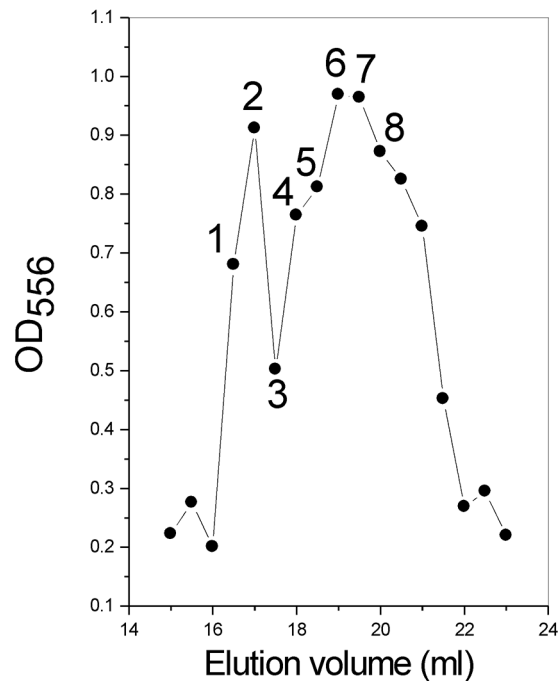
HMGA2 to produce the CTP-TMR. The CTP-TMR was incubated with HMGA2 Δ 95–108 and subjected to a pre-equilibrated gel filtration column. Fig 6 shows the elution profile of the gel filtration experiment. Our results demonstrated that the CTP-TMR was co-eluted with HMGA2 Δ 95–108. Interestingly, there are two co-elution peaks (Fig 6). Possibly, the first peak represents two CTP-TMR molecules binding to one HMGA2 Δ 95–108 and the second peak represents one CTP-TMR molecule binding to one HMGA2 Δ 95–108. An alternative possibility would be that the first peak contains one molecule of the CTP-TMR binding to two molecules of HMGA2 Δ 95–108 and the second peak corresponds to one molecule of the CTP-TMR binding to one molecule of HMGA2 Δ 95–108. Further studies are required to determine the binding stoichiometry.

Discussion

HMGA2, a member of the HMGA family [46] is a classic example of IDP [39,47–49]. It has a characteristic of low overall hydrophobicity and high net charge [48]. Hydrodynamic properties obtained from gel-filtration (Fig 1C) and sedimentation velocity studies (Table 1) showed that HMGA2 is an unfolded, extended, and non-globular protein (Table 2). CD and NMR spectroscopic measurements reveal little secondary or tertiary structure [29]. The key discovery of this study is that HMGA2 is a homodimer under physiological conditions. Not only was a significant amount of HMGA2 cross-linked into dimers by a zero length chemical cross-linker, EDC (Fig 2), but also results from several biophysical methods, such as sedimentation velocity, FRET, and mass spectrometry, demonstrated that it is a stable homodimer in aqueous buffer solution (Figs 3 and 4 and Table 1). An intriguing and important question is: how could an intrinsically unstructured HMGA2 gain quaternary structure, i.e. form homodimers?

Our preliminary results showed that the quaternary structure stems from electrostatic interactions between the positively charged “AT-hooks” and the negatively charged C-terminus. As described above, the charge distribution of HMGA2 is asymmetrical (Fig 1A). This unique

A



B

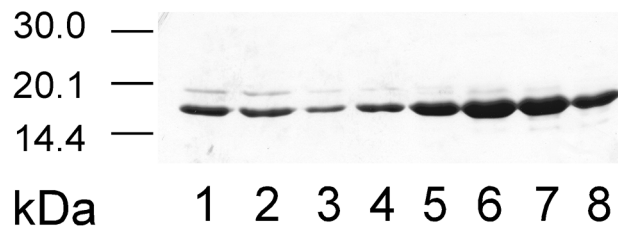


Fig 6. The CTP-TMR and HMGA2Δ95–108 co-eluting in gel-filtration chromatography. The CTP-TMR was prepared as described under “Materials and Methods” and incubated with HMGA2Δ95–108 at 24°C for 30 min in BPES buffer. The CTP-TMR and HMGA2Δ95–108 mixture was then subjected to a Sephacryl S-100 HR filtration column (1×50 cm) equilibrated with BPES buffer. Gel filtration profile of the CTP-TMR binding to HMGA2Δ95–108 was monitored by a graph of OD₅₅₆ versus elution volume (A) and a 15% SDS PAGE gel (B). Lanes 1 to 8 of the SDS-PAGE gel (B) correspond to the fractions 1 to 8 labeled in panel a. Free HMGA2Δ95–108 and the CTP-TMR were eluted at 22 and 30 ml respectively in the column.

doi:10.1371/journal.pone.0130478.g006

property provides an opportunity for the protein to self-associate. As demonstrated in Fig 5, HMGA2Δ94–108, a mutant protein without the negatively charged C-terminus, cannot be cross-linked into dimers by EDC. The CTP containing the negatively charged C-terminus tightly binds to HMGA2Δ94–108 (Fig 6). Moreover, we showed that the negatively charged C-terminus binds to the second “AT-hook” (data not shown) therefore promoting the dimer formation. A possible mechanism would be that the dimer association process is initiated by the charge neutralization and subsequently enforced by the hydrophobic interaction and hydrogen bonding from the peptide backbone. Fig 7 is a schematic graph explaining this mechanism.

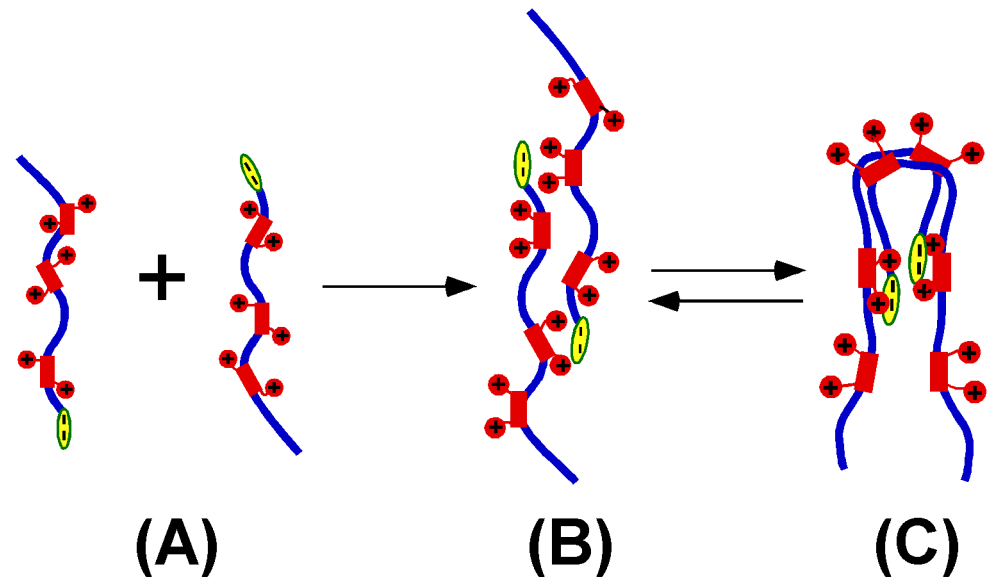


Fig 7. A possible model for the HMGA2 homodimerization. Blue lines represent the protein backbone. Electrostatic interactions between the positively charged “AT hooks” (red rectangle with two red circles) and the negatively charged C-terminus (yellow oval) coordinate the dimer formation. **(A)** represents HMGA2 monomers. **(B)** and **(C)** represent different interchangeable conformations of HMGA2 homodimers. **(C)** is more consistent with our EDC cross-linking and sedimentation velocity results. The HMGA2 homodimers may be an ensemble of different conformers.

doi:10.1371/journal.pone.0130478.g007

The “unstructured” monomers (Fig 7A) interact with each other to form a homodimer (Fig 7B and 7C) through electrostatic interactions between the highly charged “AT-hooks” (red rectangle with two red circles) and the highly charged C-terminus (yellow oval). The homodimers do not have regular secondary structure and are composed of an ensemble of different conformers with distinct and dynamic angles [39,47,50]. They may have local and limited residual structure that is critical for self-association. This dimerization process is reminiscent of the initial step of the amyloid aggregation of a large number of neurodegenerative diseases including Alzheimer’s disease and Parkinson’s disease. In these cases the proteins change their random coil to amyloidogenic β -sheet conformation therefore leading to self-association [51–53]. As demonstrated previously, any generic proteins including intrinsically unstructured proteins have the potential to form amyloid aggregates under suitable conditions [54,55]. This property results from the inherent physicochemical properties of the polypeptide backbone (hydrophobicity and hydrogen bonding) rather than the specific interaction between the side chains [54,56,57]. Although charge was considered to be the key parameter to prevent protein association or aggregation [58], HMGA2 has an asymmetrical charge distribution that would promote self-association. Indeed, recent evidence showed that the electrostatic interaction can promote protein or polypeptide’s self-association. Tjernberg *et al.* [59] showed that peptides as few as 4 residues can form well defined amyloid fibril. Both charge attraction and hydrophobic interaction are required. Goers *et al.* showed that several unstructured polycations, such as spermine, polylysine, polyarginine, and polyethyleneimine tightly bind to α -synuclein, an IDP, and catalyze its oligomerization [60]. This process was mediated by the electrostatic interaction between the negatively charged C-terminus and the polycations, and may be enforced by the hydrophobic interaction and hydrogen bonding of the peptide backbone [48]. These studies suggest that the intrinsically “unstructured” proteins or polypeptides can interact with each other to form higher structures.

Our conclusion that HMGA2 is a homodimer in solution is further supported by previous observations. Yie *et al.* showed that HMGA1a, another member of HMGA family, interacts with itself in a glutathione S-transferase (GST)-pull down experiment and the minimal region required for the self-association contains the last basic repeat and the acidic C-terminus (Fig 1 of reference [61]). The self-association may be entirely caused by the electrostatic interaction between the unstructured “AT hooks” and the C-terminus; however, a possible involvement of the well-folded GST in the pull-down experiment would complicate the interpretation of the results. In a separate study, Padmanabhan *et al.* demonstrated that *Myxococcus xanthus* transcription factor CarD, a HMGA-like protein containing both the “AT-hook” DNA-binding domain and the acidic regions, is a homodimer [62]. Sedimentation equilibrium analysis confirmed that CarD is a homodimer. However, because “the inherent difficulty in pinpointing the mechanism of HMGA cooperativity has been noted before and attributed to, among others, its lack of defined structures [62],” it is difficult to determine whether the “AT hooks” and the acidic domain were involved in the dimer formation. In contrast, this study implied that the unstructured “AT-hooks” were not required for the dimer formation. Here, using several biochemical and biophysical methods we demonstrated that the “AT-hook” DNA binding proteins, although without a defined secondary or tertiary structure, form higher structures such as homodimers.

It has been demonstrated recently that other IDPs are also capable of self-associating into homodimers [63–67]. For instance, the cytoplasmic region of the T cell receptor subunit, an IDP is able to self-associate into homodimers [63]. Interestingly, NMR studies showed that the dimerization was not accompanied by a disorder-to-order transition, suggesting that specific interactions exist between two unstructured subunits [68]. Another example is the intrinsically disordered N-terminal domain of ultraspirale from *Aedes aegypti* (aaUsp-NTD) [67]. In solution, it self-associated into homodimers as well [67]. It is possible that many other IDPs can self-associate into homodimers and the homodimerization is critical for their biological functions.

As mentioned above, HMGA2 is a DNA-binding protein and specifically recognizes the minor groove of AT-rich DNA sequences. Since many promoter regions usually contain multiple AT-rich sites [69,70]. It is possible that HMGA2 cooperatively binds to these regions as a homodimer, and thus modulates the DNA conformation, providing a framework for organizing functional transcription machinery.

Supporting Information

S1 Fig. A plot of the individual fits of the sedimentation velocity data to the model of a single ideal species by the program Sedanal (version 3.45). Panels A to C represent the sedimentation velocity experiments performed for HMGA2 concentrations of 135, 45, and 13.5 μM , respectively. The sedimentation velocity results are shown by the black dotted lines plotted as the concentration difference between pairs of interference scans against radial distance. The red curves are calculated fits. The blue lines are the residuals. Fifty pairs of scans were used in the fitting but only three pairs are shown.

(TIF)

S1 Table. Secondary structure fractions of HMGA2 analyzed by three software programs, CONTIN, CDSSTR, and SELCON3.

(DOCX)

S2 Table. Results for individually fitting the sedimentation velocity data to the model of a single ideal species by the program Sedanal (version 3.45).
(DOCX)

Acknowledgments

We thank Drs. Jonathan B. Chaires (University of Louisville), Watson Lees (Florida International University), and Roger McMacken (Johns Hopkins University) for their comments to improve the paper. We also thank Dr. James Potter (University of Miami) for use of the CD spectrometer in his laboratory and Drs. James Cole and Jeff Lary at the University of Connecticut Biotechnology Center for performing sedimentation velocity experiments.

Author Contributions

Conceived and designed the experiments: FF-L FL. Performed the experiments: LF MAMB CH AG. Analyzed the data: FF-L FL. Wrote the paper: FF-L FL.

References

1. Zhou X, Benson KF, Ashar HR, Chada K (1995) Mutation responsible for the mouse pygmy phenotype in the developmentally regulated factor HMGI-C. *Nature* 376: 771–774. PMID: [7651535](#)
2. Hauke S, Leopold S, Schlueter C, Flohr AM, Murua EH, Rogalla P et al. (2005) Extensive expression studies revealed a complex alternative splicing pattern of the HMGA2 gene. *Biochim Biophys Acta* 1729: 24–31. PMID: [15882911](#)
3. Anand A, Chada K (2000) In vivo modulation of Hmgic reduces obesity. *Nat Genet* 24: 377–380. PMID: [10742101](#)
4. Alonso N, Guillen R, Chambers JW, Leng F (2015) A rapid and sensitive high-throughput screening method to identify compounds targeting protein-nucleic acids interactions. *Nucleic Acids Res.*
5. Goodwin G (1998) The high mobility group protein, HMGI-C. *Int J Biochem Cell Biol* 30: 761–766. PMID: [9722980](#)
6. Reeves R (2003) HMGA proteins: flexibility finds a nuclear niche? *Biochem Cell Biol* 81: 185–195. PMID: [12897853](#)
7. Morishita A, Zaidi MR, Mitoro A, Sankarasharma D, Szabolcs M, Okada Y et al. (2013) HMGA2 is a driver of tumor metastasis. *Cancer Res* 73: 4289–4299. doi: [10.1158/0008-5472.CAN-12-3848](#) PMID: [23722545](#)
8. Fedele M, Battista S, Manfioletti G, Croce CM, Giaccotti V, Fusco A (2001) Role of the high mobility group A proteins in human lipomas. *Carcinogenesis* 22: 1583–1591. PMID: [11576996](#)
9. Ligon AH, Morton CC (2000) Genetics of uterine leiomyomata. *Genes Chromosomes Cancer* 28: 235–245. PMID: [10862029](#)
10. Schoenmakers EF, Wanschura S, Mols R, Bullerdiek J, Van den BH, Van de Ven WJ (1995) Recurrent rearrangements in the high mobility group protein gene, HMGI-C, in benign mesenchymal tumours. *Nat Genet* 10: 436–444. PMID: [7670494](#)
11. Rogalla P, Drechsler K, Schroder-Babo W, Eberhardt K, Bullerdiek J (1998) HMGIC expression patterns in non-small lung cancer and surrounding tissue. *Anticancer Res* 18: 3327–3330. PMID: [9858904](#)
12. Winslow MM, Dayton TL, Verhaak RG, Kim-Kiselak C, Snyder EL, Feldser DM et al. (2011) Suppression of lung adenocarcinoma progression by Nkx2-1. *Nature* 473: 101–104. doi: [10.1038/nature09881](#) PMID: [21471965](#)
13. Kumar MS, Armenteros-Monterroso E, East P, Chakravorty P, Matthews N, Winslow MM et al. (2014) HMGA2 functions as a competing endogenous RNA to promote lung cancer progression. *Nature* 505: 212–217. doi: [10.1038/nature12785](#) PMID: [24305048](#)
14. Sun M, Song CX, Huang H, Frankenberger CA, Sankarasharma D, Gomes S et al. (2013) HMGA2/TET1/HOXA9 signaling pathway regulates breast cancer growth and metastasis. *Proc Natl Acad Sci U S A* 110: 9920–9925. doi: [10.1073/pnas.1305172110](#) PMID: [23716660](#)
15. Muller MH, Drieschner N, Focken T, Bartnitzke S, Winter N, Klemke M et al. (2013) HMGA2 expression in the PC-3 prostate cancer cell line is autonomous of growth factor stimulation. *Anticancer Res* 33: 3069–3078. PMID: [23898062](#)

16. Efanov A, Zanesi N, Coppola V, Nuovo G, Bolon B, Wernicle-Jameson D et al. (2014) Human HMGA2 protein overexpressed in mice induces precursor T-cell lymphoblastic leukemia. *Blood Cancer J* 4: e227. doi: [10.1038/bcj.2014.46](https://doi.org/10.1038/bcj.2014.46) PMID: [25014774](https://pubmed.ncbi.nlm.nih.gov/25014774/)
17. Abe N, Watanabe T, Sugiyama M, Uchimura H, Chiappetta G, Fusco A et al. (1999) Determination of high mobility group I(Y) expression level in colorectal neoplasias: a potential diagnostic marker. *Cancer Res* 59: 1169–1174. PMID: [10096541](https://pubmed.ncbi.nlm.nih.gov/10096541/)
18. Meyer B, Loeschke S, Schultze A, Weigel T, Sandkamp M, Goldmann T et al. (2007) HMGA2 overexpression in non-small cell lung cancer. *Mol Carcinog*.
19. Fusco A, Fedele M (2007) Roles of HMGA proteins in cancer. *Nat Rev Cancer* 7: 899–910. PMID: [18004397](https://pubmed.ncbi.nlm.nih.gov/18004397/)
20. Miao Y, Cui T, Leng F, Wilson WD (2008) Inhibition of high-mobility-group A2 protein binding to DNA by netropsin: a biosensor-surface plasmon resonance assay. *Anal Biochem* 374: 7–15. PMID: [18023407](https://pubmed.ncbi.nlm.nih.gov/18023407/)
21. Weedon MN, Lettre G, Freathy RM, Lindgren CM, Voight BF, Perry JR et al. (2007) A common variant of HMGA2 is associated with adult and childhood height in the general population. *Nat Genet* 39: 1245–1250. PMID: [17767157](https://pubmed.ncbi.nlm.nih.gov/17767157/)
22. Horikoshi M, Yaghoobkar H, Mook-Kanamori DO, Sovio U, Taal HR, Hennig BJ et al. (2013) New loci associated with birth weight identify genetic links between intrauterine growth and adult height and metabolism. *Nat Genet* 45: 76–82. doi: [10.1038/ng.2477](https://doi.org/10.1038/ng.2477) PMID: [23202124](https://pubmed.ncbi.nlm.nih.gov/23202124/)
23. Copley MR, Babovic S, Benz C, Knapp DJ, Beer PA, Kent DG et al. (2013) The Lin28b-let-7-Hmga2 axis determines the higher self-renewal potential of fetal haematopoietic stem cells. *Nat Cell Biol* 15: 916–925. doi: [10.1038/ncb2783](https://doi.org/10.1038/ncb2783) PMID: [23811688](https://pubmed.ncbi.nlm.nih.gov/23811688/)
24. Stein JL, Medland SE, Vasquez AA, Hibar DP, Senstad RE, Winkler AM et al. (2012) Identification of common variants associated with human hippocampal and intracranial volumes. *Nat Genet* 44: 552–561. doi: [10.1038/ng.2250](https://doi.org/10.1038/ng.2250) PMID: [22504417](https://pubmed.ncbi.nlm.nih.gov/22504417/)
25. Wolffe AP (1994) Architectural transcription factors. *Science* 264: 1100–1101. PMID: [8178167](https://pubmed.ncbi.nlm.nih.gov/8178167/)
26. Cui T, Wei S, Brew K, Leng F (2005) Energetics of binding the mammalian high mobility group protein HMGA2 to poly(dA-dT)₂ and poly(dA)-poly(dT). *J Mol Biol* 352: 629–645. PMID: [16109425](https://pubmed.ncbi.nlm.nih.gov/16109425/)
27. Fonfria-Subiros E, Acosta-Reyes F, Saperas N, Pous J, Subirana JA, Campos JL (2012) Crystal structure of a complex of DNA with one AT-hook of HMGA1. *PLoS One* 7: e37120. doi: [10.1371/journal.pone.0037120](https://doi.org/10.1371/journal.pone.0037120) PMID: [22615915](https://pubmed.ncbi.nlm.nih.gov/22615915/)
28. Huth JR, Bewley CA, Nissen MS, Evans JN, Reeves R, Gronenborn AM et al. (1997) The solution structure of an HMG-I(Y)-DNA complex defines a new architectural minor groove binding motif. *Nat Struct Biol* 4: 657–665. PMID: [9253416](https://pubmed.ncbi.nlm.nih.gov/9253416/)
29. Cui T, Joynt S, Morillo V, Baez M, Hua Z, Wang X et al. (2007) Large scale preparation of the mammalian high mobility group protein A2 for biophysical studies. *Protein Pept Lett* 14: 87–91. PMID: [17266655](https://pubmed.ncbi.nlm.nih.gov/17266655/)
30. Cui T, Leng F (2007) Specific recognition of AT-rich DNA sequences by the mammalian high mobility group protein AT-hook 2: a SELEX study. *Biochemistry* 46: 13059–13066. PMID: [17956125](https://pubmed.ncbi.nlm.nih.gov/17956125/)
31. Chen B, Young J, Leng F (2010) DNA bending by the mammalian high-mobility group protein AT hook 2. *Biochemistry* 49: 1590–1595. doi: [10.1021/bi901881c](https://doi.org/10.1021/bi901881c) PMID: [20108983](https://pubmed.ncbi.nlm.nih.gov/20108983/)
32. Laue TM, Shah BD, Ridgeway TM, Pelletier SL (1992) Analytical Ultracentrifugation in Biochemistry and Polymer Science. 99–125.
33. Fernandez-Lima FA, Kaplan DA, Park MA (2011) Note: Integration of trapped ion mobility spectrometry with mass spectrometry. *Rev Sci Instrum* 82: 126106. doi: [10.1063/1.3665933](https://doi.org/10.1063/1.3665933) PMID: [22225261](https://pubmed.ncbi.nlm.nih.gov/22225261/)
34. Fernandez-Lima F, Kaplan DA, Suetering J, Park MA (2011) Gas-phase separation using a trapped ion mobility spectrometer. *Int J Ion Mobil Spectrom* 14. doi: [10.1007/s12127-011-0067-8](https://doi.org/10.1007/s12127-011-0067-8) PMID: [24163587](https://pubmed.ncbi.nlm.nih.gov/24163587/)
35. Schenk ER, Ridgeway ME, Park MA, Leng F, Fernandez-Lima F (2014) Isomerization kinetics of AT hook decapeptide solution structures. *Anal Chem* 86: 1210–1214. doi: [10.1021/ac403386q](https://doi.org/10.1021/ac403386q) PMID: [24364733](https://pubmed.ncbi.nlm.nih.gov/24364733/)
36. Schenk ER, Mendez V, Landrum JT, Ridgeway ME, Park MA, Fernandez-Lima F (2014) Direct observation of differences of carotenoid polyene chain cis/trans isomers resulting from structural topology. *Anal Chem* 86: 2019–2024. doi: [10.1021/ac403153m](https://doi.org/10.1021/ac403153m) PMID: [24428664](https://pubmed.ncbi.nlm.nih.gov/24428664/)
37. Hernandez DR, Debord JD, Ridgeway ME, Kaplan DA, Park MA, Fernandez-Lima F (2014) Ion dynamics in a trapped ion mobility spectrometer. *Analyst* 139: 1913–1921. doi: [10.1039/c3an02174b](https://doi.org/10.1039/c3an02174b) PMID: [24571000](https://pubmed.ncbi.nlm.nih.gov/24571000/)
38. Earl Wadsworth McDaniel and Edward Allen Mason (1973) The mobility and diffusion of ions in gases. New York: John Wiley and Sons. 372 p.

39. Dunker AK, Lawson JD, Brown CJ, Williams RM, Romero P, Oh JS et al. (2001) Intrinsically disordered protein. *J Mol Graph Model* 19: 26–59. PMID: [11381529](#)
40. Ward JJ, McGuffin LJ, Bryson K, Buxton BF, Jones DT (2004) The DISOPRED server for the prediction of protein disorder. *Bioinformatics* 20: 2138–2139. PMID: [15044227](#)
41. Linding R, Russell RB, Neduva V, Gibson TJ (2003) GlobPlot: Exploring protein sequences for globularity and disorder. *Nucleic Acids Res* 31: 3701–3708. PMID: [12824398](#)
42. Sreerama N, Woody RW (2000) Estimation of protein secondary structure from circular dichroism spectra: comparison of CONTIN, SELCON, and CDSSTR methods with an expanded reference set. *Anal Biochem* 287: 252–260. PMID: [11112271](#)
43. Reeves R (2001) Molecular biology of HMGA proteins: hubs of nuclear function. *Gene* 277: 63–81. PMID: [11602345](#)
44. Schuck P (2000) Size-distribution analysis of macromolecules by sedimentation velocity ultracentrifugation and lamm equation modeling. *Biophys J* 78: 1606–1619. PMID: [10692345](#)
45. Stafford WF, Sherwood PJ (2004) Analysis of heterologous interacting systems by sedimentation velocity: curve fitting algorithms for estimation of sedimentation coefficients, equilibrium and kinetic constants. *Biophys Chem* 108: 231–243. PMID: [15043932](#)
46. Bustin M (2001) Revised nomenclature for high mobility group (HMG) chromosomal proteins. *Trends Biochem Sci* 26: 152–153. PMID: [11246012](#)
47. Wright PE, Dyson HJ (1999) Intrinsically unstructured proteins: re-assessing the protein structure-function paradigm. *J Mol Biol* 293: 321–331. PMID: [10550212](#)
48. Uversky VN (2002) Natively unfolded proteins: a point where biology waits for physics. *Protein Sci* 11: 739–756. PMID: [11910019](#)
49. Hansen JC, Lu X, Ross ED, Woody RW (2006) Intrinsic protein disorder, amino acid composition, and histone terminal domains. *J Biol Chem* 281: 1853–1856. PMID: [16301309](#)
50. Fink AL (2005) Natively unfolded proteins. *Curr Opin Struct Biol* 15: 35–41. PMID: [15718131](#)
51. Hardy J, Selkoe DJ (2002) The amyloid hypothesis of Alzheimer's disease: progress and problems on the road to therapeutics. *Science* 297: 353–356. PMID: [12130773](#)
52. Dobson CM (2004) Principles of protein folding, misfolding and aggregation. *Semin Cell Dev Biol* 15: 3–16. PMID: [15036202](#)
53. Thirumalai D, Klimov DK, Dima RI (2003) Emerging ideas on the molecular basis of protein and peptide aggregation. *Curr Opin Struct Biol* 13: 146–159. PMID: [12727507](#)
54. Guijarro JI, Sunde M, Jones JA, Campbell ID, Dobson CM (1998) Amyloid fibril formation by an SH3 domain. *Proc Natl Acad Sci U S A* 95: 4224–4228. PMID: [9539718](#)
55. Litvinovich SV, Brew SA, Aota S, Akiyama SK, Haudenschild C, Ingham KC (1998) Formation of amyloid-like fibrils by self-association of a partially unfolded fibronectin type III module. *J Mol Biol* 280: 245–258. PMID: [9654449](#)
56. Stefani M, Dobson CM (2003) Protein aggregation and aggregate toxicity: new insights into protein folding, misfolding diseases and biological evolution. *J Mol Med* 81: 678–699. PMID: [12942175](#)
57. Linding R, Schymkowitz J, Rousseau F, Diella F, Serrano L (2004) A comparative study of the relationship between protein structure and beta-aggregation in globular and intrinsically disordered proteins. *J Mol Biol* 342: 345–353. PMID: [15313629](#)
58. Chiti F, Calamai M, Taddei N, Stefani M, Ramponi G, Dobson CM (2002) Studies of the aggregation of mutant proteins in vitro provide insights into the genetics of amyloid diseases. *Proc Natl Acad Sci U S A* 99 Suppl 4: 16419–16426. PMID: [12374855](#)
59. Tjernberg L, Hosia W, Bark N, Thyberg J, Johansson J (2002) Charge attraction and beta propensity are necessary for amyloid fibril formation from tetrapeptides. *J Biol Chem* 277: 43243–43246. PMID: [12215440](#)
60. Goers J, Uversky VN, Fink AL (2003) Polycation-induced oligomerization and accelerated fibrillation of human alpha-synuclein in vitro. *Protein Sci* 12: 702–707. PMID: [12649428](#)
61. Yie J, Merika M, Munshi N, Chen G, Thanos D (1999) The role of HMG I(Y) in the assembly and function of the IFN-beta enhanceosome. *EMBO J* 18: 3074–3089. PMID: [10357819](#)
62. Padmanabhan S, Elias-Arnanz M, Carpio E, Aparicio P, Murillo FJ (2001) Domain architecture of a high mobility group A-type bacterial transcriptional factor. *J Biol Chem* 276: 41566–41575. PMID: [11533063](#)
63. Sigalov A, Aivazian D, Stern L (2004) Homooligomerization of the cytoplasmic domain of the T cell receptor zeta chain and of other proteins containing the immunoreceptor tyrosine-based activation motif. *Biochemistry* 43: 2049–2061. PMID: [14967045](#)

64. Danielsson J, Liljedahl L, Barany-Wallje E, Sonderby P, Kristensen LH, Martinez-Yamout MA et al. (2008) The intrinsically disordered RNR inhibitor Sml1 is a dynamic dimer. *Biochemistry* 47: 13428–13437. PMID: [19086274](#)
65. Lanza DC, Silva JC, Assmann EM, Quaresma AJ, Bressan GC, Torriani IL et al. (2009) Human FEZ1 has characteristics of a natively unfolded protein and dimerizes in solution. *Proteins* 74: 104–121. doi: [10.1002/prot.22135](#) PMID: [18615714](#)
66. Simon SM, Sousa FJ, Mohana-Borges R, Walker GC (2008) Regulation of Escherichia coli SOS mutagenesis by dimeric intrinsically disordered umuD gene products. *Proc Natl Acad Sci U S A* 105: 1152–1157. doi: [10.1073/pnas.0706067105](#) PMID: [18216271](#)
67. Pieprzyk J, Zbela A, Jakob M, Ozyhar A, Orłowski M (2014) Homodimerization propensity of the intrinsically disordered N-terminal domain of Ultraspiracle from *Aedes aegypti*. *Biochim Biophys Acta* 1844: 1153–1166. doi: [10.1016/j.bbapap.2014.03.010](#) PMID: [24704038](#)
68. Sigalov AB, Zhuravleva AV, Orekhov VY (2007) Binding of intrinsically disordered proteins is not necessarily accompanied by a structural transition to a folded form. *Biochimie* 89: 419–421. PMID: [17174464](#)
69. Whitley MZ, Thanos D, Read MA, Maniatis T, Collins T (1994) A striking similarity in the organization of the E-selectin and beta interferon gene promoters. *Mol Cell Biol* 14: 6464–6475. PMID: [7523851](#)
70. Foti D, Iuliano R, Chiefari E, Brunetti A (2003) A nucleoprotein complex containing Sp1, C/EBP beta, and HMGI-Y controls human insulin receptor gene transcription. *Mol Cell Biol* 23: 2720–2732. PMID: [12665574](#)